

Indirect determination of the missing energy content in extensive air showers

H.M.J. Barbosa, F. Catalani, J. A. Chinellato, C. Dobrigkeit

January 10, 2019

Abstract

We used the CORSIKA simulation program to study the contribution of different components of an air shower to the total energy deposit and we present the results for different angles and primary particles. We have also calculated the amount of missing energy and parametrized the fraction E_{cal}/E_0 as a function of E_{cal} . Our results show that this parametrization varies less than 0.7% with angle or observation level. The dependence with the primary mass is less than 5.5% and, with the high energy interaction model, less than 2.3%.

1 Introduction

Numerous efforts are currently being undertaken to detect ultra high energy cosmic rays (UHECR), as they will give information not available before about the universe. Most of the new experiments are based on the fluorescence technique using the atmosphere as a calorimeter to measure the longitudinal development of air showers. Therefore, their energy reconstruction relies on the knowledge of the energy dissipated in the atmosphere through ionization and on the amount of missing energy.

As the shower develops through the atmosphere, most of its energy is deposited in the air, and a small fraction of it is emitted as fluorescence light. Nevertheless, not all the primary energy is deposited in the calorimeter. Muons and neutrinos can carry away a significant fraction of the shower energy while traversing the atmosphere almost unaffected. Since the calorimetric energy (E_{cal}) is estimated through the light profile measured by the fluorescence telescopes, the fraction of the primary energy carried by neutrinos, muons and hadrons to ground level cannot be tracked.

This fraction of the primary energy, that cannot be seen by the fluorescence telescopes, is the missing energy (E_{miss}). The amount of missing energy as a function of the calorimetric energy was initially evaluated by J.Linsley [1, 2, 3] and the Fly's Eye group [4]. More recently it was recalculated with simulations by C.Song et al [5].

In this paper we used the CORSIKA simulation program to study the contribution of different components of an air shower to the total energy deposit for different angles and primary particles. With this information, we calculated the amount of missing energy and indirectly parametrized the fraction E_{cal}/E_0 as a function of E_{cal} . We also studied the dependence of this parametrization on the the high energy interaction model and observation level.

The outline of this paper is as follows: in section 3 we discuss the concept of missing energy and give the prescription we used to calculate it. Section 2 gives a brief description of the simulations we performed. We present in section 4 a summary of all the longitudinal energy deposit profiles generated in the simulations and we discuss the missing energy correction curve obtained. Our final conclusions are presented in section 5.

2 Simulation

The CORSIKA [6] simulation code version 6.20 was used to study the energy deposit of air showers in the atmosphere. This Monte Carlo package is designed to simulate extensive air showers, up to the highest energies, and it is able to track, in great detail, all particles.

Particularly, the program provides longitudinal development tables for the energy deposit as a function of the atmospheric depth [7]. For each kind of particle (gamma, electron, muon, hadron and neutrino), the energy lost by ionization in air and simulation cuts (angle and energy thresholds) are specified. There is also information about the amount of energy carried by particles hitting the ground.

In this paper, QGSJET01 [8, 9] has been employed for higher energies $E_{lab} > 80\text{GeV}$, and GHEISHA [10] for lower energies. Optimum [11, 12] thinning [13] was applied, so as to reduce CPU time, while keeping the simulation detailed enough for our purposes. We have used a thinning level of 10^{-4} , with maximum weight limitation set to $10^{-4}E_0/\text{GeV}$ for electromagnetic particles, and $10^{-6}E_0/\text{GeV}$ for muons and hadrons.

The energy threshold for electromagnetic particles was set to 50keV and, for hadrons and muons, 50MeV . Ground level was fixed to 1400m .

Proton and Iron initiated air showers were simulated for energies between $10^{18} - 10^{20}\text{eV}$ and four different angles 0° , 30° , 45° and 60° . For each combination of these parameters, 100 shower simulations were performed, and the mean longitudinal profiles of energy deposit were carefully studied.

With the angle fixed at 45° , we have also simulated proton and iron showers with a different high energy interaction model (sibyll2.1) and detection level (near sea level).

3 Missing Energy

In order to evaluate the amount of missing energy in air showers we have used the mean longitudinal profiles of energy deposit present in the CORSIKA output.

As monte carlo codes are not able to follow all low energy particles in detail, due to CPU time requirements, we need to consider what happens with low energy particles in the atmosphere, i.e., how should we treat the energy carried by gammas, electrons, muons and hadrons not tracked due to the simulation cuts.

For the low energy electromagnetic particles, we made the assumption that all the energy is deposited, since only electromagnetic processes are significant.

The low energy muons will decay emitting one electron and two neutrinos. Hence the energy is divided approximately equally between them. Therefore, we consider that

1/3 of the energy of low energy muons, not tracked by the Monte-Carlo, is deposited in the air. The other 2/3 contribute to the missing energy.

For the hadrons, we follow Gaisser [14] and consider the same partition of energy used for the muons. This is so because they will decay emitting pions, subsequently leading to muons or gammas.

Therefore, in the next sections, the prescription used for calculating the missing energy is as follows:

$$E_{miss} = E_\nu + \frac{2}{3}E_\mu^{air-cut} + \frac{2}{3}E_{hadr}^{air-cut} + E_\mu^{grd-cut} + E_{hadr}^{grd-cut} \quad (1)$$

where E_ν is the energy carried away by neutrinos and the other terms refer to muons and hadrons dropped from the simulation. The indexes air-cut refer to the angular and energy cuts in the atmosphere. The indexes grd-cut refer to the energy carried by particles to observation level.

Since $E_0 = E_{miss} + E_{cal}$, we can indirectly calculate the fraction of the calorimetric energy measured with the fluorescence telescopes by:

$$\frac{E_{cal}}{E_0} = 1 - \frac{E_{miss}}{E_0} \quad (2)$$

4 Results

For clarity, we present in this section the results from our simulations. In table 1 we show, for each simulated angle and energy, the contribution for the energy deposit from different shower components, as a percentage of the primary energy.

Each three lines, corresponding to a fixed choice of angle and energy, discriminate three different contributions for the energy deposit, which we have called: (ION) ionization in air, (CUT) simulation cuts and (GRD) particles arriving at ground. Each column gives the contribution from different shower components: gammas, electrons, muons, hadrons and neutrinos. The first value (first/second) refers to proton primaries, while the second refers to iron primaries.

The first line accounts for ionization energy losses in air, and hence we have no contributions from gammas or neutrinos. We have considered all such contributions as calorimetric energy (see equation 1).

The second line gives the total energy of particles left out of the simulations because of angular or energy cuts. Since particles being emitted upward must have very low energy (though not as low as the simulation energy threshold), we applied the prescription given in section 3. Hence, all energy from gammas and electrons not followed by the monte carlo, were considered as calorimetric energy. For muons and hadrons, 2/3 were counted as missing energy. Since neutrinos are not tracked in the simulation, they are dropped as soon as produced. That is why we have all their contributions in the second line (cuts). We have considered all their energy as missing energy.

The last line gives the amount of energy carried by particles arriving at the observation level. In this case we have considered all energy from gammas and electrons hitting the ground as calorimetric energy. It has to be so, because they are accounted for when evaluating the track length integral of the reconstructed charged particle profile, to find the calorimetric energy. For muons and hadrons, we have considered all the energy arriving on the ground as missing energy.

4.1 Missing energy

We have used the data in table 1 to evaluate the mean missing energy for each combination of angle, energy and primary particle as given by equations 1 and 2.

In the upper panel of figure 1, the correction factor for the missing energy is shown, plotted as the fraction E_{cal}/E_0 , as a function of E_{cal} . We can see that the variation in the amount of missing energy is only slightly dependent on the angle. At $10^{19}eV$, the ratio E_{cal}/E_0 varies between $91.0 - 91.2\%$ for protons, and between $87.4 - 87.8\%$ for iron. Even at other energies, where we found a stronger dependence, the variation is less than 0.7% .

On the other hand, the ratio E_{cal}/E_0 is largely dependent on the primary mass. At a fixed angle, the difference in the amount of missing energy for proton and iron induced air showers decreases with energy. For instance, at 45° this difference is $5.5\%/10^{18}eV$, $3.8\%/10^{19}eV$ and $2.5\%/10^{20}eV$.

Therefore, the total systematic error while calculating the primary energy with a mean curve, for iron and proton, and a fixed angle is less than $\pm 2.8\% \pm 0.4\%$. In table 2, we give the fitting parameters of the mean missing energy correction function for different simulations conditions. For 45° showers, this is:

$$\frac{E_{cal}}{E_0} = 0.952 - 0.082 \frac{E_{cal}}{1EeV}^{-0.154} \quad (3)$$

The lower panel of figure 1 shows in detail the mean missing energy correction (50%proton + 50%iron). As can be noticed, there is only a small shift in the curves relative to the previous result by Song et al. Both results agree to within 0.8%, but the simulations were not carried under the same conditions and should not be compared directly. On figure 2 (upper panel) we compare, for 45° , the missing energy correction curves obtained with the ground level set to $1400m$ and $110m$, which compares well with the $300m$ used by C.Song et al. As can be seen, the 0.8% difference is due to the observation level change.

We found a much more strong dependence with the interaction model, as shown in the lower panel of figure 2. We compared, for proton and iron at 45° , the missing energy correction curves obtained with QGSJET01 and Sibyll2.1 [15] models. The difference is practically constant: around 2.3% for proton and 2.2% for iron. In all case, sibyll predicts less missing energy than qgsjet.

5 Conclusions

Although we have used an indirect and completely new way of calculating the fraction E_{cal}/E_0 , our result agrees with the previous calculation of Song et al, within the simulation limits.

We have found that the missing energy content in extensive air showers varies less than 0.7% with angle or observation level. The dependence with the primary mass is less than 5.5% and, with the high energy interaction model, less than 2.3%.

Therefore, we estimate that the total systematical error introduced by the use of just one parametrization of the missing energy correction curve, for a mixture of proton and iron, is below 3%.

Acknowledgments

The authors would like to thank B. Dawson and C. Song for the fruitful discussions.

References

- [1] J. Linsley. In *18th Int. Cosmic Ray Conf.*, volume 12, pages 135–138. Bangalore, India, August 22 - September 3 1983.
- [2] J. Linsley. In *19th Int. Cosmic Ray Conf.*, volume 7, pages 167–170. La Jolla, USA, NASA, August 11-23 1985.
- [3] J. Linsley. In *19th Int. Cosmic Ray Conf.*, volume 2, pages 154–157. La Jolla, USA, NASA, August 11-23 1985.
- [4] R. M. Baltrusaitis et al. In *19th Int. Cosmic Ray Conf.*, volume 7, pages 159–163. La Jolla, USA, NASA, August 11-23 1985.
- [5] C. Song et al. *Astropart. Phys.*, 14:7, 2000.
- [6] D. Heck et al. Fzka 6019. Technical report, Forschungszentrum Karlsruhe, www-ik.fzk.de/heck/corsika, 1998.
- [7] D. Heck M. Risse. submitted to Astroparticle Physics, 2003, arXiv:astro-ph/0308158v1.
- [8] A. I. Pavlov N. N. Kalmykov, S. S. Ostapchenko. *Nucl. Phys. B (Proc. Suppl.)*, 52B:17, 1997.
- [9] D. Heck et al. In *Proc. 27th Int. Cosmic Ray Conf. Hamburg (Germany)*, volume 1, page 233, 2001.
- [10] H. Fesefeldt. Report pitha-85/02. Technical report, RWTH Aachen, 1985.
- [11] M. Kobal for the Pierre Auger Collaboration. *Astropart. Phys.*, 15:259, 2001.
- [12] M. Risse et al. In *Proc. 27th Int. Cosmic Ray Conf. Hamburg (Germany)*, volume 2, page 522, 2001.
- [13] A. M. Hillas. *Nucl. Phys. B (Proc. Suppl.)*, 52B:29, 1997.
- [14] T. K. Gaisser. Cambridge University Press, 1990.
- [15] R. S. Fletcher et al. *Phys. Rev. D*, (50):5710, 1994.

| | | | gammas | electrons | muons | hadrons | neutrinos |
|-------|--------|-----|-------------|-------------|-----------|-----------|-----------|
| 0deg | 1EeV | ION | - / - | 45.3 / 52.1 | 0.7 / 1.2 | 0.3 / 0.4 | - / - |
| | | CUT | 0.8 / 0.9 | 7.3 / 8.5 | 0.1 / 0.1 | 1.6 / 2.3 | 2.6 / 4.1 |
| | | GRD | 16.1 / 10.0 | 17.7 / 10.2 | 4.8 / 7.5 | 2.7 / 2.7 | - / - |
| | 10EeV | ION | - / - | 40.6 / 47.7 | 0.6 / 0.8 | 0.2 / 0.3 | - / - |
| | | CUT | 0.7 / 0.8 | 6.5 / 7.7 | 0.1 / 0.1 | 1.3 / 1.8 | 2.0 / 3.0 |
| | | GRD | 19.5 / 14.2 | 22.5 / 15.1 | 3.7 / 5.6 | 2.4 / 2.8 | - / - |
| | 100EeV | ION | - / - | 35.5 / 42.3 | 0.5 / 0.6 | 0.2 / 0.2 | - / - |
| | | CUT | 0.6 / 0.7 | 5.7 / 6.8 | 0.0 / 0.1 | 1.1 / 1.4 | 1.6 / 2.3 |
| | | GRD | 22.3 / 18.0 | 26.9 / 20.4 | 3.1 / 4.3 | 2.5 / 2.8 | - / - |
| 30deg | 1EeV | ION | - / - | 56.8 / 59.4 | 0.9 / 1.4 | 0.3 / 0.4 | - / - |
| | | CUT | 1.1 / 1.1 | 10.5 / 11.0 | 0.1 / 0.1 | 1.8 / 2.8 | 2.9 / 4.6 |
| | | GRD | 9.4 / 5.1 | 9.6 / 4.8 | 5.1 / 7.9 | 1.5 / 1.5 | - / - |
| | 10EeV | ION | - / - | 54.1 / 58.3 | 0.7 / 1.1 | 0.2 / 0.3 | - / - |
| | | CUT | 1.0 / 1.1 | 9.9 / 10.8 | 0.1 / 0.1 | 1.6 / 2.1 | 2.3 / 3.5 |
| | | GRD | 11.9 / 7.6 | 12.6 / 7.5 | 4.1 / 6.0 | 1.4 / 1.5 | - / - |
| | 100EeV | ION | - / - | 50.6 / 55.5 | 0.6 / 0.8 | 0.2 / 0.3 | - / - |
| | | CUT | 0.9 / 1.0 | 9.2 / 10.2 | 0.1 / 0.1 | 1.3 / 1.7 | 2.0 / 2.7 |
| | | GRD | 14.4 / 10.5 | 16.0 / 10.9 | 3.5 / 4.7 | 1.3 / 1.5 | - / - |
| 45deg | 1EeV | ION | - / - | 66.9 / 63.7 | 1.2 / 1.7 | 0.3 / 0.4 | - / - |
| | | CUT | 1.4 / 1.4 | 14.6 / 13.9 | 0.1 / 0.1 | 2.1 / 2.8 | 3.5 / 5.2 |
| | | GRD | 2.2 / 1.2 | 1.9 / 1.1 | 5.4 / 8.1 | 0.5 / 0.5 | - / - |
| | 10EeV | ION | - / - | 66.8 / 65.7 | 1.0 / 1.4 | 0.3 / 0.3 | - / - |
| | | CUT | 1.4 / 1.4 | 14.5 / 14.4 | 0.1 / 0.1 | 1.9 / 2.4 | 2.8 / 4.0 |
| | | GRD | 3.4 / 2.0 | 3.0 / 1.7 | 4.4 / 6.2 | 0.5 / 0.5 | - / - |
| | 100EeV | ION | - / - | 65.0 / 66.3 | 0.8 / 1.1 | 0.2 / 0.3 | - / - |
| | | CUT | 1.4 / 1.4 | 14.1 / 14.4 | 0.1 / 0.1 | 1.6 / 2.0 | 2.4 / 3.2 |
| | | GRD | 5.2 / 3.0 | 5.0 / 2.7 | 3.7 / 5.0 | 0.5 / 0.5 | - / - |
| 60deg | 1EeV | ION | - / - | 66.3 / 61.8 | 1.5 / 2.1 | 0.3 / 0.4 | - / - |
| | | CUT | 1.7 / 1.6 | 18.8 / 17.6 | 0.1 / 0.1 | 2.0 / 2.6 | 4.0 / 5.9 |
| | | GRD | 0.1 / 0.1 | 0.1 / 0.1 | 5.2 / 7.9 | 0.1 / 0.0 | - / - |
| | 10EeV | ION | - / - | 67.9 / 64.7 | 1.2 / 1.7 | 0.2 / 0.3 | - / - |
| | | CUT | 1.7 / 1.6 | 19.3 / 18.4 | 0.1 / 0.1 | 1.8 / 2.3 | 3.3 / 4.6 |
| | | GRD | 0.1 / 0.1 | 0.1 / 0.1 | 4.3 / 6.1 | 0.1 / 0.0 | - / - |
| | 100EeV | ION | - / - | 68.9 / 66.8 | 1.1 / 1.4 | 0.2 / 0.3 | - / - |
| | | CUT | 1.7 / 1.7 | 19.6 / 19.0 | 0.1 / 0.1 | 1.7 / 2.0 | 2.8 / 3.7 |
| | | GRD | 0.1 / 0.1 | 0.1 / 0.1 | 3.7 / 4.8 | 0.1 / 0.1 | - / - |

Table 1: Mean energy deposit contributions (in percentage of primary's energy) from different shower components. Each three lines correspond to a fixed choice of angle and energy, and discriminate: (ION) ionization in air, (CUT) simulation cuts and (GRD) particles arriving at ground. The first value (first/second) refers to proton while the second refers to iron.

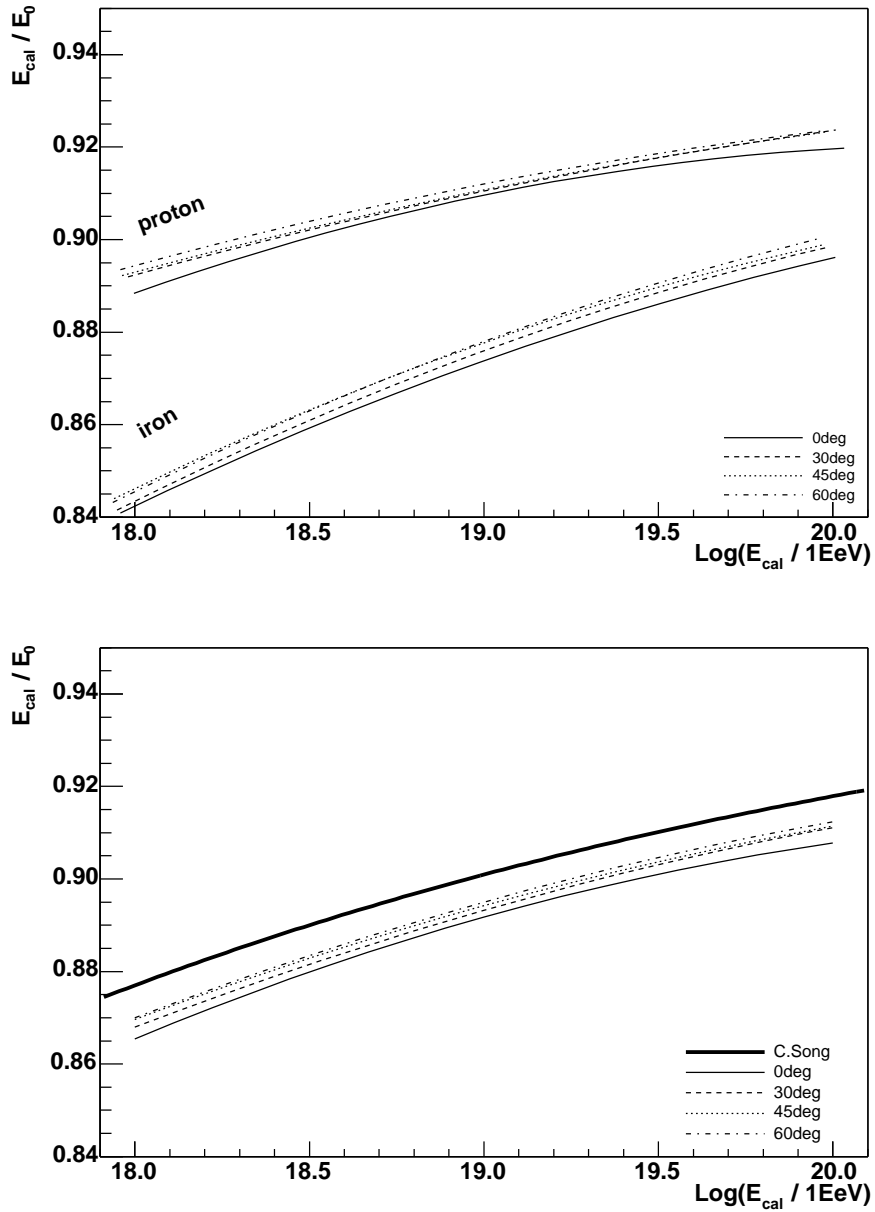


Figure 1: Upper Panel: Missing energy correction plotted as the fraction E_{cal}/E_0 as a function of E_{cal} . Proton and iron showers at four different angles. Lower Panel: The mean between iron and proton missing energy correction is plotted together with C.Song result.

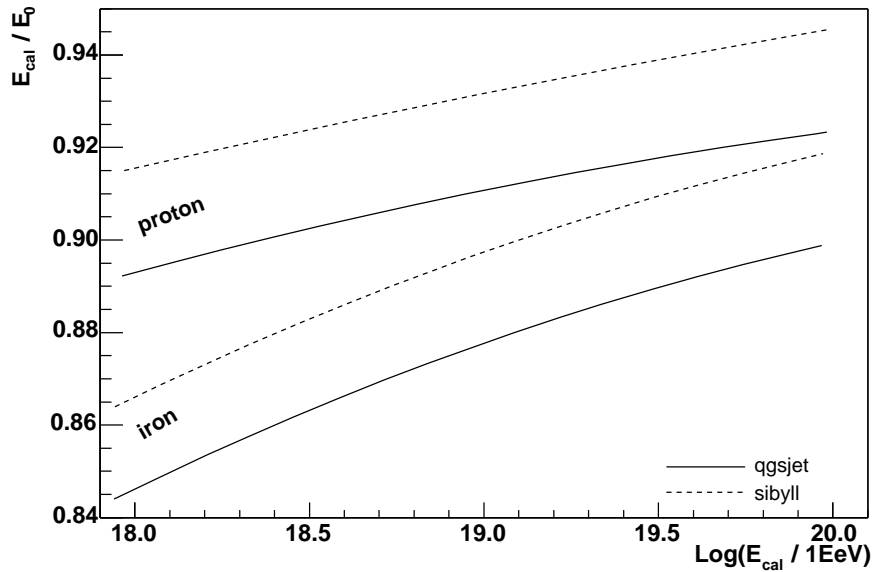
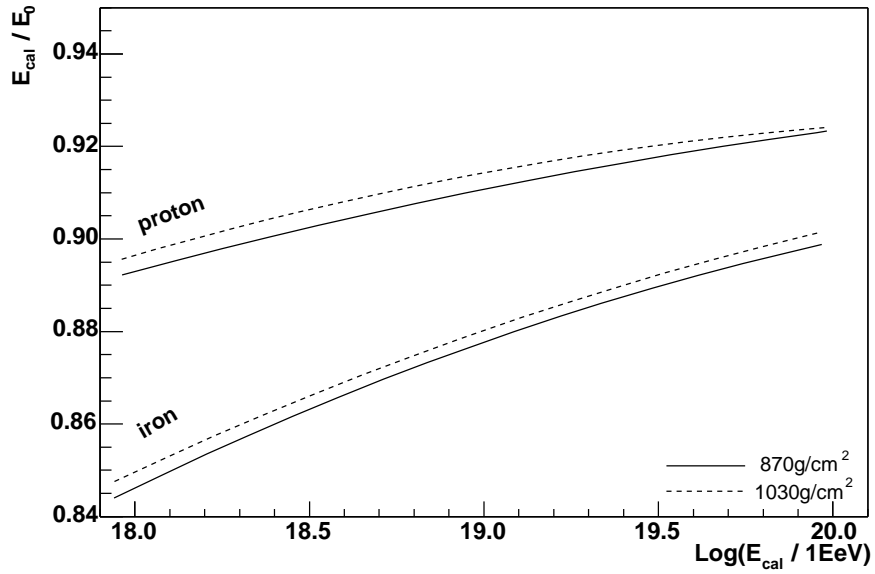


Figure 2: Missing energy correction plotted as the fraction E_{cal}/E_0 as a function of E_{cal} . For proton and iron primaries at 45° it is shown the variation with ground level (upper Panel) and high energy interaction model (lower Panel).

Coefficients of correction function

| angle | Iron | | | Iron/Proton | | | Proton | | |
|-------|-------|-------|-------|--------------|--------------|--------------|--------|-------|-------|
| | A | B | C | A | B | C | A | B | C |
| 0deg | 0.950 | 0.107 | 0.150 | 0.933 | 0.067 | 0.215 | 0.928 | 0.040 | 0.333 |
| 30deg | 0.951 | 0.108 | 0.155 | 0.954 | 0.087 | 0.150 | 0.958 | 0.065 | 0.141 |
| 45deg | 0.947 | 0.101 | 0.162 | 0.952 | 0.082 | 0.154 | 0.956 | 0.063 | 0.142 |
| 60deg | 0.957 | 0.111 | 0.150 | 0.952 | 0.082 | 0.158 | 0.947 | 0.053 | 0.175 |

Table 2: Fitting parameters for different simulation conditions, as plotted in figure 1. The mid column indicates the 50%/50% mixture and the values corresponding to 45° are bold faced. The fit function used was: $A - B(E/EeV)^{-C}$.